Binding of IgG to MoFcγRII Purified and Reconstituted into Supported Planar Membranes As Measured by Total Internal Reflection Fluorescence Microscopy†

Claudia L. Poglitsch, Martina T. Sumner, and Nancy L. Thompson*
Department of Chemistry, University of North Carolina at Chapel Hill, Chapel Hill, North Carolina 27599-3290
Received December 28, 1990; Revised Manuscript Received April 10, 1991

ABSTRACT: Total internal reflection fluorescence microscopy (TIRFM) has been combined with functional reconstitution of the mouse IgG receptor moFcγRII in substrate-supported planar membranes to quantitatively probe IgG–moFcγRII interactions. MoFcγRII was purified from the macrophage-related cell line J774A.1 using affinity chromatography with Fab fragments of the anti-moFcγRII monoclonal antibody 2.4G2. Purified moFcγRII was reconstituted into liposomes by detergent dialysis, and the liposomes were fused on quartz substrates to form supported planar membranes containing moFcγRII. TIRFM measurements showed that fluorescently labeled 2.4G2 Fab specifically bound to the planar membranes, confirming the presence of moFcγRII. The receptor density in the planar membranes was sufficiently high to allow direct detection of bound, fluorescently labeled polyclonal and monoclonal mouse IgG with TIRFM, demonstrating that moFcγRII retained Fc-mediated IgG binding activity after planar membrane formation and permitting direct measurement of bound IgG as a function of the IgG solution concentration. Cross-inhibition measurements showed that polyclonal mouse IgG blocked the binding of labeled 2.4G2 Fab and that 2.4G2 Fab blocked the binding of labeled polyclonal IgG. This work provides a direct measure of the relatively weak IgG–moFcγRII association constant and demonstrates a new model system in which the chemical and physical properties of IgG–moFcγRII interactions can be quantitatively characterized as a function of membrane, antibody, and solution properties.

Cell surface receptors for the Fc region of antibodies are found on a number of immunological cell types, including macrophages, lymphocytes, natural killer cells, basophils, mast cells, and polymorphonuclear leukocytes. A range of different antibody receptors with distinct antibody class and subclass specificities have been identified. By linking the cellular and humoral immune responses, these receptors play key roles in antibody-mediated cellular immune mechanisms such as phagocytosis, B cell activation and regulation, cellular degranulation, and antibody-dependent cell-mediated cytotoxicity.

One Fc receptor that has been extensively studied is the mouse IgG receptor moFcγRII, which is expressed in relatively abundant amounts on macrophages and some lymphocytes (Unkeless et al., 1988). Biochemical and immunological characterization of moFcγRII has been facilitated by the development of a hybridoma that secretes monoclonal antibodies specific for the receptor (2.4G2) (Unkeless, 1979) and by subsequent receptor purification (Mellman & Unkeless, 1980) and cDNA cloning and sequencing (Hibbs et al., 1986; Ravetch et al., 1986; Lewis et al., 1986). MoFcγRII is a glycosylated, single-transmembrane polypeptide belonging to the immunoglobulin supergene family (Hibbs et al., 1988; Mellman et al., 1988). Radioimmune assays have shown that moFcγRII binds monomeric IgG1, IgG2b, and possibly IgG2a with low affinity and aggregated IgG1, IgG2b, and IgG2a with higher affinity (Unkeless et al., 1988; Weinshank et al., 1988; Burton, 1985). MoFcγRII occurs in at least three isoforms, called α, β_1, and β_2 (Ravetch et al., 1986).

Physical characterization of IgG–moFcγRII interactions has been complicated by the weak association of monomeric IgG with moFcγRII (Dower et al., 1981; Segal & Titus, 1978) and by the presence of other cell surface IgG receptors (Unkeless et al., 1988). The relationship of the thermodynamic and kinetic aspects of IgG–moFcγRII interactions, the translational and rotational mobilities of moFcγRII and IgG–moFcγRII complexes, and the interactions of moFcγRII or IgG–moFcγRII complexes with other cell surface or circulating molecules to the immune functions in which the different forms of moFcγRII participate are not yet well understood. Elucidation of these different physical phenomena may lead to an increased understanding of the mechanics of signal generation and transduction for the moFcγRII receptor and may serve as a paradigm for other receptor-mediated processes. The molecular details of the association of IgG with moFcγRII are also of importance in the development and application of biosensors and immunodiagnostic devices.

A recently developed method for quantitatively investigating interactions between protein ligands and cell surface receptors is to combine total internal reflection fluorescence microscopy (TIRFM)[1] with substrate-supported planar phospholipid membranes. Supported planar membranes have previously been used to examine a diverse array of membrane processes (Thompson & Palmer, 1988; McConnell et al., 1986). One method of forming supported membranes that contain reconstituted transmembrane proteins is to fuse liposomes that contain the proteins at solid surfaces. This approach has been used to functionally reconstitute the mouse histocompatibility antigens H-2K^k (Brian & McConnell, 1984) and I-A^d (Watts et al., 1984) and the insulin receptor (Sui et al., 1988). With

† This work was supported by National Institutes of Health Grant GM-37145 and National Science Foundation Presidential Young Investigator Award DCB-8552986.
* To whom correspondence should be addressed.

[1] Abbreviations: TIRFM, total internal reflection fluorescence microscopy; DNP, dinitrophenyl; R-, tetramethylrhodamine isothiocyanate labeled; F-, fluorescein isothiocyanate labeled; PBS, phosphate-buffered saline; BCA, bicinchoninic acid; TFA, trifluoroacetic acid; NBD-PE, 1-acyl-2-[12-[(7-nitro-2,1,3-benzoxadiazol-4-yl)amino]dodecanoyl]-phosphatidylethanolamine; BSA, bovine serum albumin; FPPR, fluorescence pattern photobleaching recovery.

0006-2960/91/0430-6662$02.50/0

use of TIRFM (Hellen et al., 1988; Lanni et al., 1985; Axelrod et al., 1984), a laser beam that is internally reflected at the membrane/solution interface creates an evanescent field that penetrates approximately 850 Å into the solution and selectively excites membrane-bound fluorescent ligands. TIRFM has recently been used to examine the association at equilibrium of a variety of biological molecules with specific surface sites (Pisarchick & Thompson, 1990; Kalb et al., 1990; Sui et al., 1988; Watts et al., 1986; Weis et al., 1982) and is one of only a few techniques available for quantitatively characterizing weak interactions between protein ligands and receptors.

In an earlier work, TIRFM was used to investigate the specific association of IgG with supported planar membranes containing moFcγRII that were formed from membrane fragments isolated from a macrophage-related cell line (Poglitsch & Thompson, 1990). However, the moFcγRII surface density was low so that bound, fluorescently labeled IgG could not be readily detected with a reasonable signal-to-noise ratio, and the IgG binding activity of moFcγRII in the planar membranes was demonstrated only by competitive schemes with fluorescently labeled anti-moFcγRII antibodies. Described in this paper is the application of TIRFM to substrate-supported planar membranes that contain purified and functionally reconstituted moFcγRII. The membranes have a significantly higher moFcγRII density, allowing direct detection of fluorescently labeled polyclonal and monoclonal mouse IgG. The results demonstrate a new model system in which the thermodynamic and kinetic aspects of IgG–moFcγRII interactions can be quantitatively characterized as a function of membrane, antibody, and solution properties.

Materials and Methods

Cells. The macrophage-related cell line J774A.1, which contains cell surface moFcγRII, was obtained from the University of North Carolina Tissue Culture Facility. The rat–mouse hybidoma 2.4G2, which secretes antibodies specific for moFcγRII, and the mouse–mouse hybridoma ANO2, which secretes anti–dinitrophenyl (DNP) mouse IgG1, were obtained as gifts from Prof. Betty Diamond of the Albert Einstein College of Medicine and from Prof. Harden McConnell of Stanford University, respectively. Cells were maintained in culture as previously described [J774A.1 and 2.4G2, Poglitsch and Thompson (1990); ANO2, Wright et al. (1988)] except that J774A.1 cells were grown in spinner flasks.

Antibodies. Intact mouse IgG, mouse IgG $F(ab)'_2$, rat IgG Fab, and (alkaline phosphatase)-conjugated goat anti-(rat IgG) were obtained commercially (Jackson ImmunoResearch, Inc., West Grove, PA). 2.4G2 antibodies were purified from cell supernatants by affinity chromatography with an anti-(rat IgG κ light chain) antibody (MAR18.5) and 2.4G2 Fabs were produced and purified as described (Poglitsch & Thompson, 1990). ANO2 antibodies were isolated from cell supernatants by affinity chromatography with DNP-conjugated human serum albumin (Pisarchick & Thompson, 1990).

Antibodies were labeled with tetramethylrhodamine (R-) or fluorescein (F-) isothiocyanate (Molecular Probes, Inc., Junction City, OR) (Mishell & Shiigi, 1980). Unreacted dye was removed by Sephadex G50-80 chromatography and subsequent dialysis against phosphate-buffered saline (PBS; 0.05 M sodium phosphate, 0.15 M sodium chloride, 0.01% sodium azide, pH 7.4). Labeled 2.4G2 and rat IgG Fab were further purified with MAR18.5 affinity chromatography. No unreacted fluorophore was observed at the dye front when labeled antibodies were analyzed on SDS–PAGE gels and illuminated with ultraviolet light.

Labeled and unlabeled antibodies were clarified at 100000*g* for 2 h at 4 °C before application to planar membranes. Gel filtration experiments (G200-120 Sephadex, 1.5 cm × 48 cm, 0.1 mL/min, sample volume, 1.0 mL, PBS, 25 °C) showed that labeled and unlabeled antibodies (mouse IgG and ANO2; 1.0 mg/mL) eluted with symmetrical peaks and at identical elution volumes corresponding to IgG monomers. Possible higher molecular weight IgG aggregates were not detected.

The concentrations of labeled and unlabeled antibodies and the molar ratios of fluorophore to antibody (0.8–2.0, except as noted) in clarified solution were estimated spectrophotometrically with use of assumed molar absorptivities (Timbs & Thompson, 1990). The spectrophotometrically determined R-ANO2 and R-(mouse IgG) concentrations agreed well with independent determinations using a bicinchoninic acid (BCA) assay (Pierce Chemical Co., Rockford, IL) (H. V. Hsieh, C. L. Poglitsch, and N. L. Thompson, unpublished results). The relative fluorescence intensities of different antibody preparations were estimated on a spectrofluorometer (8000C; SLM, Urbana, IL) with excitation and emission wavelengths equal to 550 and 580 nm, respectively.

MoFcγRII Purification. MoFcγRII was purified from J774A.1 cells with modifications of a previously developed procedure (Mellman & Unkeless, 1980). A total of 2×10^9 J774A.1 cells was homogenized (Wheaton 358054, Millville, N.J.) in 50 mL PBS with 0.5% Nonidet P-40, 1 mM phenylmethanesulfonyl fluoride, and 0.4 unit/mL aprotinin. The homogenate was clarified at 1600*g* for 5 min and then twice at 40000*g* for 30 min. The supernatant was carefully removed to minimize contamination by floating lipids and was applied to a 2.4G2 Fab affinity column equilibrated with wash buffer (PBS with 0.5% Nonidet P-40). The column was rinsed with 500 mL of wash buffer and then eluted with PBS containing 0.5% *n*-octyl β-D-glucopyranoside (octyl glucoside) and 0.1 M triethylamine, pH 11.5. The eluate was immediately neutralized with 1 M Tris, pH 7.4 (1/1 v/v) and dialyzed against three 100-mL volumes of HEPES buffer (0.05 M NaCl, 0.165 M sucrose, 10 mM *N*-2-hydroxyethylpiperazine-*N'*-2-ethanesulfonic acid (HEPES), 0.01% NaN_3, Tris pH 7.4) with 20 mM octyl glucoside. All procedures were carried out at 4 °C.

MoFcγRII concentrations were determined with use of the BCA assay (see above). MoFcγRII purity was monitored by 10% reducing and nonreducing SDS–PAGE with silver staining. Western blots were carried out according to the ProtoBlot protocol (Promega, Madison, WI) using Immobilon-P membranes (Millipore, Bedford, MA), 2.4G2 as the primary antibody, (alkaline phosphatase)-conjugated goat anti-(rat IgG) as the secondary antibody, and nitro blue tetrazolium/5-bromo-4-chloro-3-indolyl phosphate as the enzymatic substrate. In some cases, moFcγRII was further purified by use of analytical reverse-phase HPLC [2.1 mm × 30 mm RP300 (C_8) column from Applied Biosystems, Inc., Foster City, CA; mobile phase A, 0.1% trifluoroacetic acid (TFA)/water (v/v); mobile phase B, acetonitrile/water/TFA, 70/30/0.06 (v/v); gradient of 0% B for 5 min, 0–100% B in 45 min; peak elution, 39 min; detection wavelength, 230 nm]. The first 19 N-terminal amino acids were sequenced for the protein in the main peak (Applied Biosystems 470A protein sequencer).

Substrate-Supported Planar Membranes. Purified moFcγRII was reconstituted into lipid vesicles by detergent dialysis (Young et al., 1983a). Egg phosphatidylcholine and cholesterol (Sigma Chemical Co., St. Louis, MO), judged to be pure by thin-layer chromatography, were mixed 6/1 (w/w)

in chloroform/methanol (2/1 v/v), dried under vacuum, solubilized with ~25 μg/mL moFcγRII in HEPES buffer with 20 mM octyl glucoside at a protein/lipid ratio of 1/10 (w/w), treated for 2 min in a water-bath sonicator, and dialyzed for 72 h against four 1-L volumes of HEPES buffer. Some detergent-dialyzed liposomes contained only lipid and some were labeled with ~5 mol % 1-acyl-2-[12-[(7-nitro-2,1,3-benzoxadiazol-4-yl)amino]dodecanoyl]phosphatidylethanolamine (NBD-PE; Avanti Polar Lipids, Birmingham, AL). Liposomes derived from J774A.1 membrane fragments, with and without 5 mol % NBD-PE, were prepared as described (Poglitsch & Thompson, 1990).

Planar membranes were formed from liposomes with or without purified moFcγRII or from J774A.1 membrane fragment liposomes as described (Poglitsch & Thompson, 1990) except that substrates were washed with 3 mL of PBS after liposome adsorption. Membranes were treated with 65 μL of 10 mg/mL bovine serum albumin (BSA, Sigma) in PBS for 30 min and then with 250 μL of various antibody solutions in 5 mg/mL BSA/PBS. Planar membranes treated with fluorescently labeled antibodies were allowed to equilibrate for 30 min before microscopy measurements (except as noted). Planar membranes prepared from liposomes doped with NBD-PE were prepared in the same manner as those without NBD-PE except that the incubation step with labeled antibodies was omitted.

Fluorescence Microscopy. The fluorescence originating from labeled antibodies on planar membranes was measured at room temperature (~25 °C) with TIRFM (Axelrod et al., 1984) as described (Poglitsch & Thompson, 1990).[2] For all TIRFM data, 10 spatially independent measurements on each of 2–3 planar membranes formed from at least two separate liposome preparations were obtained. TIRFM equilibrium curves were fit to theoretical forms with use of the nonlinear curve-fitting functions in ASYST software (Asyst Software Technologies, Inc., Rochester, NY).

The lateral mobility of incorporated NBD-PE and bound F-(2.4G2 Fab) was examined with fluorescence pattern photobleaching recovery (FPPR) (Smith & McConnell, 1978) as described (Wright et al., 1988) except as follows: temperature, 25 °C; bleach pulse duration, 100–400 ms; depth of bleaching, 40–70%; radii of illuminated and observed areas, ≥150 and 38 μm, respectively; spatial periodicities in the sample plane, 16 μm (NBD-PE) or 8 μm [F-(2.4G2 Fab)]. FPPR data were analyzed as previously described (Timbs et al., 1990; Wright et al., 1988).

Results

Purification of MoFcγRII. The mouse Fc receptor moFcγRII was purified from the macrophage-related cell line J774A.1 by use of 2.4G2 Fab affinity chromatography. The eluted protein ran as a broad band of apparent molecular weight centered at about 60K on 10% SDS–PAGE gels under both nonreducing (Figure 1a) and reducing (not shown) conditions, consistent with published reports for moFcγRII (Hibbs et al., 1986). Western blot analyses of gels run under nonreducing conditions confirmed that the band migrating with apparent molecular weight ~60K was recognized by the anti-moFcγRII monoclonal antibody 2.4G2 (Figure 1b).

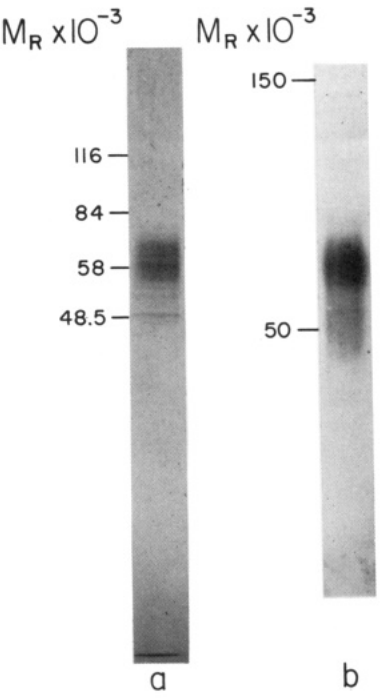

FIGURE 1: Electrophoretic mobility and Western blot analysis of purified moFcγRII. (a) Purified moFcγRII was analyzed with SDS–PAGE (10% acrylamide) under nonreducing conditions and visualized with silver staining as a broad band with apparent molecular weight centered about 60K. Low molecular weight impurities were excluded from detergent-dialyzed liposomes as judged by SDS–PAGE of reconstituted moFcγRII (not shown). (b) Purified moFcγRII on a nonreducing SDS–PAGE gel was transferred to an Immobilon-P membrane, treated with 2.4G2 IgG, and visualized with (alkaline phosphatase)-conjugated goat anti-(rat IgG).

N-Terminal amino acid sequencing showed that the first 19 amino acids of the isolated protein were identical with those of the β form of moFcγRII (Lewis et al., 1986; Ravetch et al., 1986; Hibbs et al., 1986). The N-terminal amino acid sequence does not distinguish between the moFcγRIIβ$_1$ and moFcγRIIβ$_2$ forms since they differ only in that moFcγRIIβ$_1$ contains a 47 amino acid insertion in its cytoplasmic tail (Hogarth et al., 1987; Miettinen et al., 1989). While moFcγRIIβ$_1$ appears to be absent on primary macrophages and mainly restricted to lymphocytes and lymphoid cell lines, the J774A.1 cell line may express both β isoforms (Miettinen et al., 1989; Ravetch et al., 1986). Therefore, the isolated moFcγRII was identified as primarily moFcγRIIβ and may or may not consist of a mixture of moFcγRIIβ$_1$ and moFcγRIIβ$_2$. A mixture of both β proteins could contribute to the observed broad electrophoretic mobility (Figure 1) in addition to possible heterogeneous glycosylation or differing levels of endogenous protease activity released during purification (Hunziker et al., 1990; Hibbs et al., 1988; Mellman & Unkeless, 1980). The yield of moFcγRII from 2×10^9 J774A.1 cells, as estimated from BCA protein determinations, was ~70 μg. This value is consistent with previous work (Mellman & Unkeless, 1980), assuming a moFcγRII molecular weight of 55 000 and a cell surface abundance of 500 000 per cell (Mellman & Unkeless, 1980).

[2] Previous work (Poglitsch & Thompson, 1990) has assumed an evanescent wave depth of 700 Å on the basis of the theoretical expression for the evanescent depth (Axelrod et al., 1984) and assumed refractive indices at 1.5 for the substrate and 1.334 for the solution, an incidence angle of 75°, and a vacuum wavelength of 514.5 nm. Using a more accurate value for the refractive index of fused quartz (1.467) yields a theoretical depth of 850 Å. The effect of protein concentration on the solution refractive index and hence the evanescent field depth and intensity at the interface was negligible. Assuming that the change of the solution refractive index with protein concentration was 0.185 mL/g (Sober, 1973), the largest protein concentration (5.0 mg/mL BSA and 3.0 mg/mL IgG) results in a solution refractive index increase of 0.11%. This change leads to a 1.0% increase in the evanescent field depth and a 1.1% increase in the evanescent intensity for an incident electric field perpendicular to the plane of incidence.

Table I: Lateral Mobility in Supported Planar Membranes[a]

supported planar membrane	fluorescent probe	diffusion coefficient ($\times 10^{-8}$ cm^2/s)	fractional mobility
moFcγRII(−)	NBD-PE	1.2 ± 0.1	0.57 ± 0.08
moFcγRII(+)	NBD-PE	1.9 ± 0.1	0.78 ± 0.10
J774A.1	NBD-PE	$<10^{-4}$	
moFcγRII(+)	F-(2.4G2 Fab)	$<10^{-4}$	

[a] FPPR values for the apparent diffusion coefficients and fractional mobilities are averages over 10 measurements each on three different membranes formed from at least two independent liposome preparations. Uncertainties are standard errors in the means. The value for NBD-PE in planar membranes formed from J774A.1 membrane fragment liposomes is from an earlier work (Poglitsch & Thompson, 1990).

Supported Planar Membranes. Purified moFcγRII was reconstituted into egg phosphatidylcholine/cholesterol vesicles by detergent dialysis. Previous work has shown that moFcγRII reconstituted in this manner retains the ability to bind both to 2.4G2 IgG and to immunocomplexes consisting of anti-DNP IgG bound to Sephadex coated with DNP-conjugated BSA (Young et al., 1983a). In this work, substrate-supported planar membranes containing moFcγRII [moFcγRII(+) membranes] or not containing moFcγRII [moFcγRII(−) membranes] were formed by treating fused quartz surfaces with liposome suspensions.

Epifluorescence microscopy indicated that the fluorescent lipid NBD-PE in both types of planar membranes was uniformly distributed within optical resolution except for the presence of occasional bright features of size ≤ 1 μm^2. These regions may have been due to liposomes that did not completely fuse with the bilayer or multilayer present on the surface and have been observed in similar systems (Tendian et al., 1991; Poglitsch & Thompson, 1990).

FPPR showed that the lateral mobility of the fluorescent lipid NBD-PE in both moFcγRII(+) and moFcγRII(−) membranes was high ($\sim 10^{-8}$ cm^2/s) (Table I), similar to those in other fluid-like supported planar membranes formed from detergent-dialyzed liposomes with or without transmembrane proteins (Brian & McConnell, 1984; Watts et al., 1984). The measurable long-range diffusion over distances ≥ 15 μm implies that a significant fraction of the adsorbed liposomes fuse to form a continuous substrate-supported membrane. The incomplete mobility (60–80%) may be due to incomplete surface-catalyzed fusion.

The fluorescence after photobleaching for moFcγRII(+) membranes treated with F-(2.4G2 Fab) did not significantly recover after 5 min for a spatial periodicity of 8 μm. This result assigns an upper limit of 10^{-12} cm^2/s for the apparent translational diffusion coefficient of the (2.4G2 Fab)–moFcγRII complexes with use of the functional form for FPPR data (Timbs et al., 1991; Wright et al., 1988). The low mobility of F-(2.4G2 Fab) on moFcγRII(+) membranes is consistent with results for other transmembrane proteins in similar systems (Watts et al., 1986; Brian & McConnell, 1984; Schindler et al., 1980). Although (2.4G2 Fab)–moFcγRII complexes did not exhibit measurable diffusion, membranes labeled with F-(2.4G2 Fab) appeared uniformly fluorescent, ruling out the existence of highly oligomerized receptor.

Antibody Binding to Planar Membranes Measured by TIRFM. Initial TIRFM measurements demonstrated that moFcγRII reconstituted in planar membranes retained specificity for 2.4G2 Fab and for the Fc-mediated binding of IgG (Table II): evanescently excited fluorescence intensities were much higher for R-(2.4G2 Fab) on moFcγRII(+) membranes than for R-(2.4G2 Fab) on moFcγRII(−) membranes or for R-(rat IgG) on moFcγRII(+) membranes; polyclonal mouse IgG but not polyclonal mouse IgG F(ab)′$_2$ blocked the R-(2.4G2 Fab) fluorescence on moFcγRII(+) membranes; the fluorescence of R-(mouse IgG) and R-ANO2 was much higher on moFcγRII(+) than on moFcγRII(−) membranes; the fluorescence of R-(mouse IgG) and R-ANO2 was significantly reduced in the presence of saturating amounts of unlabeled 2.4G2 Fab on moFcγRII(+) but not on moFcγRII(−) membranes; and the fluorescence of R-[mouse IgG F(ab)′$_2$] on moFcγRII(+) membranes was approximately equal to that of R-[mouse IgG F(ab)′$_2$] on moFcγRII(−) membranes in both the presence and absence of saturating amounts of 2.4G2 Fab.

The amount of R-(mouse IgG) and R-ANO2 bound to moFcγRII(+) membranes was estimated by examining the fraction of the evanescently excited fluorescence that could be photobleached (data not shown). This analysis was based on the premise that, for some evanescent intensities and bleaching durations, only surface-bound molecules are bleachable since the residency time of labeled antibodies in solution and within the evanescent field is short (< 1 ms). These measurements, obtained for several bleaching durations, showed that the fraction of fluorescence arising from bound R-(mouse IgG) and R-ANO2 on moFcγRII(+) membranes was high (≥50%), that this fraction was low (≤10%) for R-(mouse IgG) on moFcγRII(−) membranes and on moFcγRII(+) membranes in the presence of saturating concentrations of 2.4G2 Fab, and that this fraction was even lower (≤5%) for R-ANO2 on the two control samples.

For planar membranes treated with fluorescently labeled antibodies, the variation in fluorescence intensity measured over large areas (~ 1 cm^2) was small, with typical standard deviations of 1–4% for 10 measurements on a single planar

Table II: Activity and Specificity of Reconstituted MoFcγRII in Supported Planar Membranes[a]

fluorescently labeled ligand	nonfluorescent inhibitor	moFcγRII(+) membranes	moFcγRII(−) membranes
(A) 1 nM R-(2.4G2 Fab)	none	1.00 ± 0.03	0.04 ± 0.02
	10 μM mouse IgG	0.75 ± 0.02	
	10 μM mouse F(ab)′$_2$	1.06 ± 0.04	
1 nM R-(rat IgG Fab)	none	0.07 ± 0.03	0.02 ± 0.01
(B) 3 μM R-(mouse IgG)	none	1.00 ± 0.01	0.48 ± 0.01
	200 nM 2.4G2 Fab	0.44 ± 0.01	0.48 ± 0.01
3 μM R-(mouse IgG F(ab)′$_2$)	none	0.35 ± 0.01	0.36 ± 0.01
	200 nM 2.4G2 Fab	0.34 ± 0.01	0.38 ± 0.01
(C) 3 μM R-ANO2	none	1.00 ± 0.01	0.39 ± 0.01
	200 nM 2.4G2 Fab	0.34 ± 0.01	0.38 ± 0.01

[a] The binding of R-(2.4G2 Fab), R-(mouse IgG), and R-ANO2 to moFcγRII in planar membranes was characterized with TIRFM. Evanescently excited fluorescence intensities were corrected for the relative fluorescence of different labeled antibody preparations and were normalized to the fluorescence of moFcγRII(+) membranes treated with (A) R-(2.4G2 Fab), (B) R-(mouse IgG), or (C) R-ANO2. The values for the normalized fluorescence intensities are averages over 10 measurements each on three different membranes formed from at least two independent liposome preparations. Uncertainties are standard errors in the means.

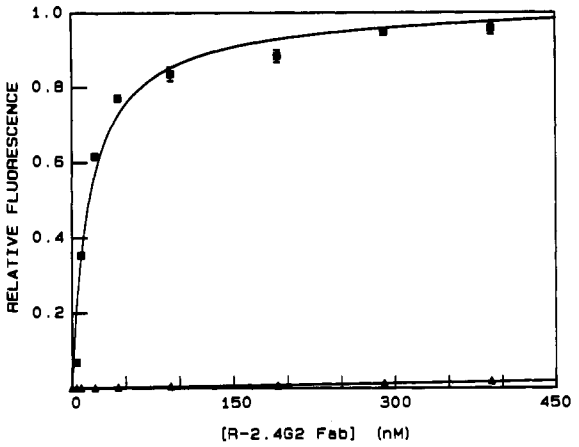

FIGURE 2: Binding of R-(2.4G2 Fab) to planar membranes. The difference (■) of the evanescently excited fluorescence of R-(2.4G2 Fab) on moFcγRII(+) membranes and moFcγRII(−) membranes (▲) increased with the R-(2.4G2 Fab) solution concentration. Comparing the data to the best fit to eq 3 (—) gave $K_a = (6.6 \pm 1.8) \times 10^7$ M^{-1}; the data are normalized so that $F(\infty) = 1.0$. The plotted solution concentrations equal the estimated values corrected for depletion (see text). Measured points represent the averages over 10 spatially independent measurements on each of three or more planar membranes.

membrane. The fluorescence of R-(mouse IgG), R-ANO2, and R-(2.4G2 Fab) on moFcγRII(+) and moFcγRII(−) membranes measured with TIRFM maintained an approximately constant value after times greater than 15 min and up to at least $2^1/_2$ h (data not shown).

The evanescently excited fluorescence of R-(2.4G2 Fab) on moFcγRII(+) membranes as a function of the solution concentration of R-(2.4G2 Fab) had the shape of a conventional adsorption isotherm whereas the fluorescence intensities of R-(2.4G2 Fab) on moFcγRII(−) membranes were negligible (Figure 2). The measured adsorption curve did not significantly change for a range of different R-(2.4G2 Fab) preparations having different fluorophore-to-antibody molar ratios (0.2–1.2). The ratio of the saturating fluorescence intensities of R-(2.4G2 Fab) on moFcγRII(+) membranes and on planar membranes made from J774A.1 membrane fragment liposomes was 41 ± 6.

The fluorescence of polyclonal R-(mouse IgG) on moFcγRII(+) membranes also increased as a function of the R-(mouse IgG) solution concentration whereas the fluorescence of R-(mouse IgG) on two different control samples, moFcγRII(−) membranes and moFcγRII(+) membranes to which saturating amounts of unlabeled 2.4G2 Fab had been added, was significantly lower and linear with concentration (Figure 3). Similar results were obtained for R-ANO2 on moFcγRII(+) membranes in the absence and presence of 2.4G2 Fab and on moFcγRII(−) membranes (Figure 4). The fluorescence intensities on the two control samples were equivalent within experimental error for both R-(mouse IgG) and R-ANO2.

The association of mouse IgG and 2.4G2 Fab with moFcγRII(+) membranes was also investigated with indirect assays in which the evanescently excited fluorescence of R-(2.4G2 Fab) in the presence of unlabeled mouse IgG, and in which the fluorescence of R-(mouse IgG) in the presence of unlabeled 2.4G2 Fab, was monitored. These measurements showed that only ~25% of the fluorescence arising from bound R-(2.4G2 Fab) could be displaced by 20 μM mouse IgG (Figure 5). This result was observed whether or not the planar membranes were preblocked with mouse IgG prior to treatment with R-(2.4G2 Fab) and mouse IgG. The fraction of

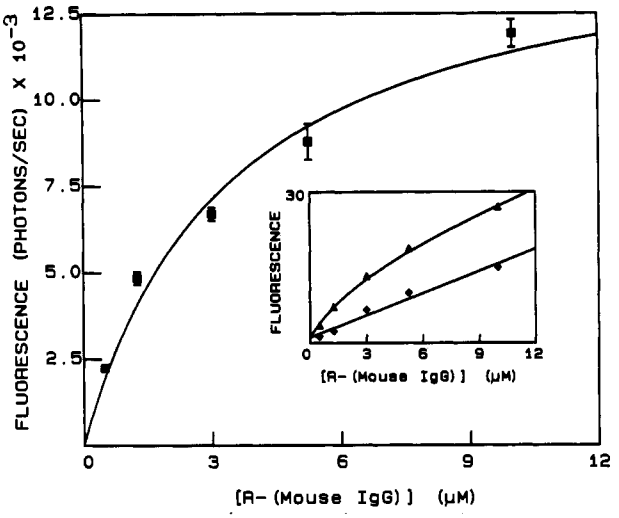

FIGURE 3: Binding of R-(mouse IgG) to planar membranes. The difference (■) of the evanescently excited fluorescence of R-(mouse IgG) on moFcγRII(+) membranes (▲) and the average of two control samples, moFcγRII(−) membranes and moFcγRII(+) membranes to which saturating amounts of unlabeled 2.4G2 Fab were added (◆), increased with the R-(mouse IgG) solution concentration. The best fit to eq 3 (—) gave $K_p = (2.9 \pm 0.4) \times 10^5$ M^{-1} and $F(\infty) = 1.5 \times 10^4$ photons/s. Uncertainties are standard errors in the means for averages over 10 spatially independent measurements on each of three planar membranes.

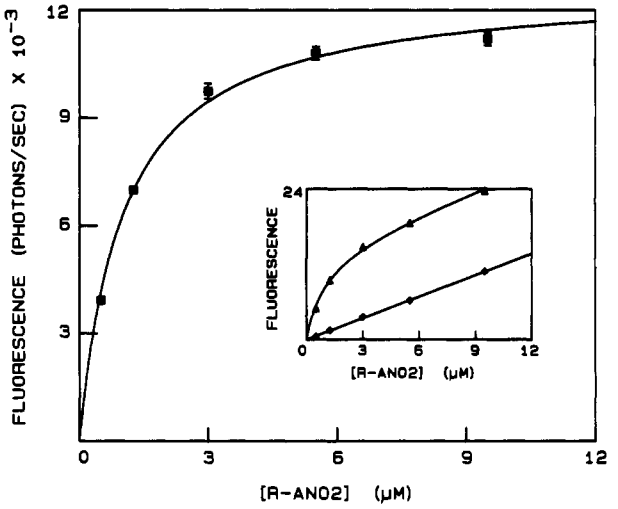

FIGURE 4: Binding of R-ANO2 to planar membranes. The difference (■) of the evanescently excited fluorescence of R-ANO2 on moFcγRII(+) membranes (▲) and the average of two control samples, moFcγRII(−) membranes and moFcγRII(+) membranes to which saturating amounts of unlabeled 2.4G2 Fab were added (◆), increased with the R-ANO2 solution concentration. Comparing the data to the best fit to eq 3 (—) gave $K_m = (9.3 \pm 0.2) \times 10^5$ M^{-1} and $F(\infty) = 1.3 \times 10^4$ photons/s. Uncertainties are standard errors in the means for averages over 10 spatially independent measurements on each of three planar membranes.

the fluorescence that could not be blocked by mouse IgG was not due to nonspecifically bound R-(2.4G2 Fab) as complete inhibition of the fluorescence could be obtained with unlabeled 2.4G2 Fab (data not shown). The 2.4G2 Fab was much more efficient at blocking R-(mouse IgG) binding to moFcγRII(+) membranes (Figure 6).

Analysis of TIRFM Binding Curves

Absolute Densities of Bound Antibodies. Antibody surface densities were estimated from the ratios (r) of the fluorescence intensities for labeled antibodies on moFcγRII(+) membranes to those on control membranes (Pisarchick & Thompson,

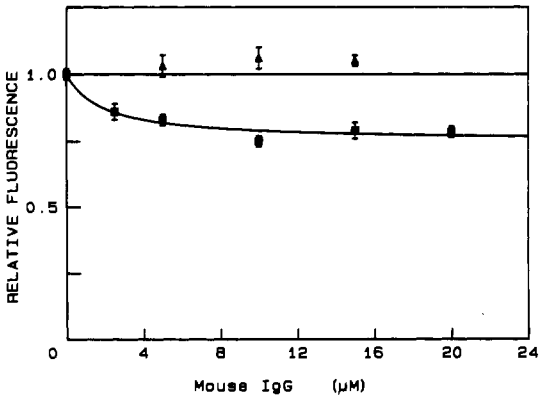

FIGURE 5: Competitive binding of R-(2.4G2 Fab) and mouse IgG to planar membranes. The fluorescence obtained with evanescent field excitation and arising from R-(2.4G2 Fab) bound to moFcγRII(+) membranes decreased as a function of the concentration of unlabeled mouse IgG (■) but remained constant as a function of the concentration of unlabeled mouse IgG F(ab)′$_2$ (▲) for applied concentrations of R-(2.4G2 Fab) equal to 1 nM. The mouse IgG data are compared to the best fit to eq 7 with use of the solution concentration corrected for depletion by membrane moFcγRII for R-(2.4G2 Fab) (0.35 nM). Uncertainties are standard errors in the means for averages over 10 spatially independent measurements on each of three planar membranes.

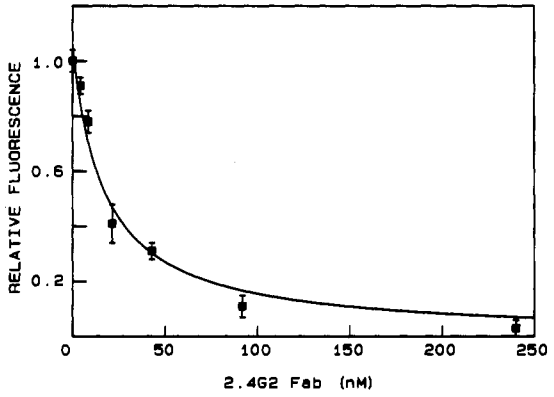

FIGURE 6: Competitive binding of R-(mouse IgG) and 2.4G2 Fab to planar membranes. The fluorescence obtained with evanescent field excitation and arising from R-(mouse IgG) bound to moFcγRII(+) membranes decreased as a function of the concentration of unlabeled 2.4G2 Fab (■) for applied concentrations of R-(mouse IgG) equal to 5 μM. The normalized fluorescence was calculated by first taking the difference between the fluorescence intensity on moFcγRII(+) membranes and moFcγRII(−) membranes and then taking the ratio of fluorescence in the presence and absence of 2.4G2 Fab. The data are compared to the best fit to eq 8 with use of the solution concentrations corrected for depletion by membrane moFcγRII for 2.4G2 Fab. Uncertainties are standard errors in the means for averages over 10 spatially independent measurements on each of two or more planar membranes.

1990). The fluorescence arising from nonspecifically adsorbed antibodies and from those excited by scattered light was small (see above). Thus, assuming no change in quantum yield upon binding

$$r \approx \frac{[S] + d[C]}{d[C]} \quad (1)$$

where [S] is the density of bound antibodies for a given antibody solution concentration [C] and d is the evanescent field depth ($\approx$ 850 Å)[2]. With use of the fractional surface site saturations β, determined as the ratios of measured fluorescence intensities at each [C] and estimated fluorescence intensities for infinite values of [C], the total antibody binding site densities were calculated as

$$[T] = [S]/\beta \approx (r - 1)d[C]/\beta \quad (2)$$

For R-(2.4G2 Fab) on moFcγRII(+) and moFcγRII(−) membranes, the measured value of r at each antibody solution concentration[3] together with the known degree of surface site saturation implied that the total surface site density of receptors that bound R-(2.4G2 Fab) in moFcγRII(+) membranes was [T] $\approx$ 1320 ± 50 molecules/μm^2. Comparing the fluorescence intensities of R-(2.4G2 Fab) on moFcγRII(+) membranes and on planar membranes made from J774A.1 membrane fragment liposomes, together with the previously measured moFcγRII density in J774A.1 planar membranes of ~50 molecules/μm^2 (Poglitsch & Thompson, 1990), gave a similar density of [T] $\approx$ 2050 ± 510 molecules/μm^2.

Use of eq 2 with the data in Figures 3 and 4 gave [T] $\approx$ 430 ± 80 molecules/μm^2 for R-(mouse IgG) and [T] $\approx$ 600 ± 25 molecules/μm^2 for R-ANO2. However, comparing the differences at saturation in the fluorescence intensities of R-(mouse IgG) and R-ANO2 on moFcγRII(+) membranes and on their control samples, normalized by the relative fluorescence intensities of R-(mouse IgG) and R-ANO2, implied that the density of R-(mouse IgG) binding sites was ~20% higher than the density of R-(ANO2) binding sites. Thus, the densities of R-(mouse IgG) and R-ANO2 binding sites on moFcγRII(+) membranes are approximately equal and about 3-fold lower than the density of R-(2.4G2 Fab) binding sites.

Basis for Equilibrium Binding Analyses. The measured total binding site densities for R-(2.4G2 Fab), R-(mouse IgG), and R-ANO2, together with the known volumes and concentrations of applied antibody solutions, the known substrate area, and the known degree of surface site saturation, were used to estimate the extent to which moFcγRII(+) membranes depleted the applied solutions of antibodies. These calculations implied that the depletion was negligible for the micromolar concentrations used with mouse IgG, mouse IgG F(ab)′$_2$, R-(mouse IgG), and R-ANO2 (≤0.2%), and the solution concentrations of these antibodies were therefore assumed to equal the applied concentrations. The estimated depletion was significant for the nanomolar concentrations used with 2.4G2 Fab and R-(2.4G2 Fab) (3–60%), and consequently the solution concentrations of these antibodies were assumed to equal the estimated values as corrected for depletion.

On moFcγRII(−) membranes and on moFcγRII(+) membranes to which saturating amounts of 2.4G2 Fab were added, the low bleachable fractions of R-(mouse IgG) and R-(ANO2) obtained with use of evanescent illumination implied that the amount of nonspecifically bound, labeled IgG was low. Thus, the nonzero fluorescence intensities for control samples arose primarily from fluorescent antibodies within the evanescent field but not bound to planar membranes. The amount of nonspecifically bound R-(2.4G2 Fab) on moFcγRII(+) membranes was also very low because negligible fluorescent intensities were measured on moFcγRII(−) membranes and for R-(rat IgG) Fab on moFcγRII(+) membranes. The small variation in fluorescence intensity measured over large areas of the planar membranes coupled with the uniform microscopic appearance of membranes containing NBD-PE or bound, fluorescently labeled antibodies suggests that the contribution to the measured fluorescence intensities from scattered excitation illumination is probably not significant. Also, the linear range of evanescently excited fluorescence as a function of

[3] For R-(2.4G2 Fab), R-(mouse IgG), and R-ANO2, estimates of the antibody surface densities were calculated only from the measured values of r where the fluorescence intensities of labeled antibodies on control planar membranes were ≥ 15% of the background fluorescence for moFcγRII(−) membranes treated with PBS.

fluorophore-labeled protein surface density extends up to at least 14 000 molecules/μm^2 (Lok et al., 1983), which is much higher than the estimated antibody surface densities at saturation on moFcγRII(+) membranes (see above). Thus, the evanescently excited fluorescence intensities, corrected for solution fluorescence, were assumed to be proportional to the surface densities of specifically bound, labeled antibodies.

The evanescently excited fluorescence intensities of labeled antibodies on planar membranes were constant after 15 min (data not shown). This result is similar to that obtained for antibodies equilibrating with hapten-conjugated phospholipids in substrate-supported monolayers (Pisarchick & Thompson, 1990; Timbs et al., 1990) and with other solid surfaces (Stenberg & Nygren, 1988; Darst et al., 1988). Along with the calibrated antibody solution concentrations and surface densities, this result supports analysis of the data in Figures 2–6 with equilibrium expressions.

Quantitative Analysis of Equilibrium Binding Curves. Apparent association constants were determined by subtracting the fluorescence intensities of samples containing only solution-phase fluorescent antibodies from those that also contained membrane-bound, fluorescent antibodies. The fluorescence differences were fit to the functional form for a reversible, bimolecular reaction, given by

$$F([C]) = \frac{F(\infty)\, K[C]}{1 + K[C]} \tag{3}$$

where [C] was the antibody solution concentration and the free parameters were the apparent association constant, K, and the fluorescence at saturation, $F(\infty)$.

Fitting the fluorescence differences for R-(2.4G2 Fab) on moFcγRII(+) membranes and moFcγRII(−) membranes to eq 3, while using the solution concentrations corrected for surface depletion (see above), gave an apparent association constant for R-(2.4G2 Fab) and moFcγRII of $K_g = (6.6 \pm 1.8) \times 10^7\ M^{-1}$ (Figure 2). The difference in the measured fluorescence intensities for polyclonal R-(mouse IgG) on moFcγRII(+) membranes and the average of two control membranes, moFcγII(−) membranes and moFcγRII(+) membranes to which a saturating amount of 2.4G2 Fab had been added, yielded an apparent association constant for R-(mouse IgG) and moFcγRII of $K_p = (2.9 \pm 0.4) \times 10^5\ M^{-1}$ (Figure 3). The fluorescence differences for monoclonal R-ANO2 on moFcγRII(+) membranes and the average of the two control membranes gave an apparent association constant for R-ANO2 and moFcγRII of $K_m = (9.3 \pm 0.2) \times 10^5\ M^{-1}$ (Figure 4).

Polyclonal mouse IgG did not completely block the fluorescence arising from R-(2.4G2 Fab) bound to moFcγRII(+) membranes (Figure 5), whereas 2.4G2 Fab did almost completely block the fluorescence arising from bound R-(mouse IgG) (Figure 6). A mechanism in which mouse IgG and 2.4G2 Fab compete for a homogeneous population of moFcγRII was thus judged to be unlikely.

One possible explanation for the data in Figure 5 is that mouse IgG does not completely inhibit the binding of R-(2.4G2 Fab) to moFcγRII. In this case, mouse IgG could reduce the apparent binding affinity of R-(2.4G2 Fab) for moFcγRII rather than completely block its binding and the fluorescence in the presence of large concentrations of unlabeled mouse IgG would not approach zero (Poglitsch & Thompson, 1990). The data in Figure 5 would be of the form

$$\frac{F_{g,p}([P])}{F_{g,p}(0)} = \frac{1 + (K_{g,p}/K_g)K_p[P]}{1 + [(1 + K_{g,p}[G])/(1 + K_g[G])]K_p[P]} \tag{4}$$

where K_g and $K_{g,p}$ are the association constants of R-(2.4G2 Fab) with free moFcγRII and with moFcγRII–IgG complexes, respectively, [G] is the R-(2.4G2 Fab) solution concentration, and [P] is the mouse IgG solution concentration. A similar and coupled behavior would also apply to the data in Figure 6, which would be of the form

$$\frac{F_{p,g}([G])}{F_{p,g}(0)} = \frac{1 + (K_{p,g}/K_p)K_g[G]}{1 + [(1 + K_{p,g}[P])/(1 + K_p[P])]K_g[G]} \tag{5}$$

where K_p and $K_{p,g}$ are the association constants of R-(mouse IgG) with free moFcγRII and with moFcγRII–(2.4G2 Fab) complexes, respectively. In addition, the four association constants would obey the relationship

$$\frac{K_{p,g}/K_p}{K_{g,p}/K_g} = 1 \tag{6}$$

Evaluation of the data in Figures 5 and 6 with eqs 4 and 5, respectively, and with K_g, K_p, [G], and [P] equal to their known values, gave $K_{g,p} = (4.9 \pm 1.8) \times 10^7\ M^{-1}$ (Figure 5) and $K_{p,g} = (-1.5 \pm 2.1) \times 10^4\ M^{-1}$ (Figure 6). The ratio in eq 6, calculated with use of these values of $K_{g,p}$ and $K_{p,g}$, $K_g = (6.6 \pm 1.8) \times 10^7\ M^{-1}$, and $K_p = (2.9 \pm 0.4) \times 10^5\ M^{-1}$, is -0.07 ± 0.10. The result that this ratio does not even approximately equal one, together with the antibody surface density data that showed that 2.4G2 Fab binding densities were ~3-fold higher than mouse IgG or ANO2 densities, argues strongly against a mechanism in which 2.4G2 Fab and mouse IgG only partially cross-inhibit binding to a homogeneous population of moFcγRII.

Another model for describing the data in Figures 5 and 6 is one in which only a fraction of the reconstituted moFcγRII that binds 2.4G2 Fab also binds the Fc region of mouse IgG and in which 2.4G2 Fab and mouse IgG bind to this fraction of moFcγRII in a mutually exclusive manner. The appropriate form for the data in Figure 5 would be

$$\frac{F_{g,p}([P])}{F_{g,p}(0)} = \left[\frac{f}{1 + [K_p[P]/(1 + K_g[G])]} + (1 - f)\right] \tag{7}$$

where the moFcγRII that binds 2.4G2 Fab is present as a fraction (f) that also binds mouse IgG and a fraction ($1 - f$) that does not bind mouse IgG. The fluorescence $F_{g,p}([P])$ ranges from $F_{g,p}(0)$ in the absence of mouse IgG to $F_{g,p}(0)(1 - f)$ in the presence of large concentrations of mouse IgG. Fitting the data in Figure 5 to eq 7 with K_g, [G], and [P] equal to their known values and $F_{g,p}(0)$, f, and K_p as free parameters yielded $f = 0.25 \pm 0.02$ and $K_p = (5.4 \pm 0.8) \times 10^5\ M^{-1}$. This value of K_p is in reasonable agreement with the directly measured value obtained from the data in Figure 3, and the value of f is consistent with the measured R-(2.4G2 Fab) and R-(mouse IgG) binding site densities.

The functional form for the inhibition of R-(mouse IgG) binding by unlabeled 2.4G2 Fab would be

$$\frac{F_{p,g}([G])}{F_{p,g}(0)} = \frac{1}{1 + [K_g[G]/(1 + K_p[P])]} \tag{8}$$

where the fluorescence $F_{p,g}([G])$ ranges from $F_{p,g}(0)$ in the absence of 2.4G2 Fab to zero in the presence of large concentrations of 2.4G2 Fab. Fitting the data in Figure 6 to eq 8 with K_p, [P], and [G] equal to their known values and $F_{p,g}(0)$ and K_g as free parameters gave a best fit with $K_g = (1.4 \pm 0.5) \times 10^8\ M^{-1}$, which is consistent with the directly measured value obtained from the data in Figure 2.

In Figure 5, as the concentration of mouse IgG is increased, less R-(2.4G2 Fab) are bound to the membrane and the solution depletion of R-(2.4G2 Fab) is potentially reduced. Quantitatively accounting for this phenomena in eq 4 and the subsequent discussion yields a value for the ratio in eq 6 equal to -0.12 ± 0.18 and does not alter the conclusion that incomplete blocking cannot explain the data in Figure 5. Accounting for this phenomena in eq 7 yields a larger value for f (≈ 0.55). In Figure 6, the amount by which the membrane depletes the solution of 2.4G2 Fab is theoretically less when some moFcγRII are occupied by R-(mouse IgG). This effect was not quantitatively considered because the solution concentration depletion of 2.4G2 Fab was negligible for all but the lowest concentration data point in Figure 6.

Discussion

Interaction of Antibodies with Planar Membranes Containing MoFcγRII. The measured value for the association constant of 2.4G2 Fab with the reconstituted moFcγRII, $K_g = (6.6 \pm 1.8) \times 10^7$ M^{-1}, is lower than the values previously measured for R-(2.4G2 Fab) on planar membranes prepared from J774A.1 membrane fragment liposomes (10^9 M^{-1}, 25 °C; Poglitsch & Thompson, 1990) and for ^{125}I-labeled (2.4G2 Fab) on J774A.1 cells (10^8–10^9 M^{-1}, 4 °C; Unkeless & Healey, 1983; Mellman & Unkeless, 1980). The 2.4G2 Fab binding to purified moFcγRII in planar membranes would be weaker than previously measured to moFcγRII in planar membranes derived from J774A.1 plasma membrane liposomes or to J774A.1 cells if moFcγRII purification resulted in loss of essential membrane components or partial moFcγRII denaturation.

The apparent association constant for mouse IgG and moFcγRII obtained from the data in Figure 3, $K_p = (2.9 \pm 0.4) \times 10^5$ M^{-1}, is to our knowledge the first reported direct measurement of this parameter. The measured value agrees with previous values obtained from indirect assays, including TIRFM measurements of the ability of unlabeled mouse IgG to block the binding of R-(2.4G2 Fab) to planar membranes constructed from J774A.1 membrane fragment liposomes ($1\text{-}5 \times 10^5$ M^{-1}, 25 °C; Poglitsch & Thompson, 1990) and radioimmune measurements of the ability of myeloma mouse IgG ($\sim 5 \times 10^5$ M^{-1}, 0 °C; Segal & Titus, 1978) and polyclonal rabbit IgG ($\sim 1.3 \times 10^6$ M^{-1}; 0 °C; Dower et al., 1981) to block the binding of ^{125}I-labeled multivalent rabbit IgG to macrophage cell surfaces. That the measured value of K_p agrees with other reports suggests that the phenomena leading to the reduced value for K_g do not significantly affect the IgG–moFcγRII interaction.

The measured value for the association constant of the mouse monoclonal IgG1 antibody ANO2 with moFcγRII obtained from the data in Figure 4, $K_m = (9.3 \pm 0.2) \times 10^5$ M^{-1}, is a factor of 3 larger than the association constant K_p for polyclonal mouse IgG. The difference between K_m and K_p may result from the heterogeneous nature of polyclonal IgG, which contains different mouse IgG subclasses that may bind to moFcγRII with a range of affinities (Unkeless et al., 1988; Weinshank et al., 1988). The average K_p might also vary between different serum samples if the IgG subclass content of the polyclonal mouse IgG differs.

The apparent association constants of mouse IgG and 2.4G2 Fab with moFcγRII do not appear to be significantly affected by the covalent attachment of tetramethylrhodamine. The values of K_p and K_g obtained for R-(mouse IgG) and R-(2.4G2 Fab) with use of direct binding measurements (Figures 3 and 2), respectively, were reasonably consistent with those obtained for mouse IgG and 2.4G2 Fab with use of indirect measurements (Figures 5 and 6), respectively. In addition, there was no significant difference between the K_g's measured directly for R-(2.4G2 Fab) on moFcγRII(+) membranes, for fluorophore-to-antibody ratios ranging from 0.2 to 1.2.

Estimates of the surface density of bound R-(2.4G2 Fab) at saturation, obtained from direct measurement of R-(2.4G2 Fab) on moFcγRII(+) membranes (~ 1320 molecules/μm^2), were similar to estimates independently obtained by comparing the fluorescence intensities of R-(2.4G2 Fab) on moFcγRII(+) membranes and on planar membranes made from J774A.1 membrane liposomes of known moFcγRII density (~ 2050 molecules/μm^2). The direct binding data for R-(mouse IgG) and R-ANO2 implied IgG surface densities of ~ 430 and ~ 600 molecules/μm^2, respectively. Use of the data in Figure 5 suggests that mouse IgG blocks only 25–50% of the bound R-(2.4G2 Fab) and implies a 2.4G2 Fab surface density of $(2\text{–}4) \times 430 \approx 860\text{–}1720$ molecules/μm^2. This result agrees well with the two other independent measures of this parameter. The moFcγRII density estimated from the known protein-to-lipid ratio and assumed surface areas of lipid (50 Å^2) and of moFcγRII (400 Å^2) is ≈ 5000 molecules/μm^2, which suggests that roughly half of the reconstituted moFcγRII are oriented with the extracellular portion of the receptor accessible to R-(2.4G2 Fab) in solution.

IgG–MoFcγRII and (2.4G2 Fab)–MoFcγRII Binding Mechanism. Although previous studies have shown that 2.4G2 Fab inhibits rosette formation between macrophages and IgG1- or IgG2b-coated erythrocytes (Unkeless, 1979), that 2.4G2 stimulates some cellular responses similar to those of moFcγRII occupied with aggregated IgG (Young et al., 1983b), and that monomeric mouse IgG can reduce the binding of 2.4G2 Fab to planar membranes constructed from macrophage membrane fragment liposomes (Poglitsch & Thompson, 1990), the precise nature of the presumably shared epitope for 2.4G2 Fab and mouse IgG is not known (Puré et al., 1987). In this work, analysis of the direct and indirect binding curves of mouse IgG and 2.4G2 Fab suggests that mouse IgG and 2.4G2 Fab inhibit binding to moFcγRII in a mutually exclusive manner. Data analysis also suggests that, in this system, only 25–50% of the moFcγRII that bind 2.4G2 Fab also bind the Fc region of mouse IgG. This interpretation is consistent with our observation that some elution buffers during affinity purification can yield moFcγRII that binds only 2.4G2 Fab (unpublished data). Taken together, the measured antibody surface densities and binding curves do not support a mechanism in which mouse IgG and 2.4G2 Fab bind to a homogeneous population of moFcγRII with incomplete blocking. However, the data do not necessarily rule out an intermediate case in which a fraction higher that 25–50% but less than 100% of the moFcγRII that bind 2.4G2 Fab also bind mouse IgG and in which the two ligands only partially block each other. In addition, other mechanistic factors such as complex IgG:moFcγRII stoichiometries (O'Grady et al., 1986), multiple association steps [e.g., Nygren and Stenberg (1989) and Pecht (1982)], or heterogeneous receptor orientations might be involved in the association of IgG with reconstituted moFcγRII.

Comparison with Planar Membranes Formed from J774A.1 Membrane Fragments. A previous work has characterized planar membranes made by treating solid supports with liposomes derived from J774A.1 membrane fragments (Poglitsch & Thompson, 1990). These planar membranes specifically bound 2.4G2 Fab and the Fc region of mouse IgG and yielded IgG–moFcγRII association constants obtained indirectly with unlabeled mouse IgG that were consistent with

the direct and indirect measurements described in this work. Advantages of planar membranes constructed from J774A.1 membrane fragment liposomes are that moFcγRII purification is not required and that more of the native membrane components are retained. However, the receptors were diluted by ~25-fold from their natural cell surface density, and the lipids were not laterally mobile. The use of liposomes containing purified moFcγRII yielded planar membranes with a much higher receptor density (similar to that found on J774A.1 cells), permitting the direct measurement of bound, labeled IgG with TIRFM. In addition, these membranes are chemically well-defined in that they contain only moFcγRII and not other IgG Fc receptors, and the receptor density and lipid composition can be systematically manipulated.

Summary. Two recently developed techniques, the formation of substrate-supported planar phospholipid membranes and total internal reflection fluorescence microscopy, have been combined and used to quantitatively characterize the relatively weak interactions of IgG with the mouse Fc receptor moFcγRII. This work adds to the currently small number of transmembrane proteins that have been functionally reconstituted into substrate-supported planar membranes and suggests that fusion of proteoliposomes to solid surfaces may be a widely applicable approach for reconstituting different transmembrane proteins. In addition, the ability of TIRFM to directly detect fluorescently labeled IgG bound to moFcγRII provides a basis for the use of dynamic techniques in TIRFM such as fluorescence photobleaching recovery and correlation spectroscopy (Tilton et al., 1990; Palmer & Thompson, 1989; Thompson & Axelrod, 1983; Burghardt & Axelrod, 1981). Steady-state TIRFM and also TIRFM with these dynamic techniques should allow characterization of new physical aspects of IgG–moFcγRII interactions such as the role of antibody and membrane structure and solution composition in IgG–moFcγRII equilibria and kinetics.

ACKNOWLEDGMENTS

We thank Russell Henry of the Protein Chemistry Laboratory of UNCCH–NIEHS for assistance with protein sequencing, Helen Hsieh and Tanya Page of the University of North Carolina for providing biochemical materials and for permission to quote unpublished results, Betty Diamond of the Albert Einstein College of Medicine for 2.4G2 hybridoma cells, and Harden McConnell of Stanford University for ANO2 hybridoma cells.

REFERENCES

Axelrod, D., Burghardt, T. P., & Thompson, N. L. (1984) *Annu. Rev. Biophys. Bioeng. 13*, 247.

Brian, A. A., & McConnell, H. M. (1984) *Proc. Natl. Acad. Sci. U.S.A. 81*, 6159.

Burghardt, T. P., & Axelrod, D. (1981) *Biophys. J. 33*, 455.

Burton, D. R. (1985) *Mol. Immunol. 22*, 161.

Darst, S. A., Robertson, C. R., & Berzofsky, J. A. (1988) *Biophys. J. 53*, 533.

Dower, S. K., DeLisi, C., Titus, J. A., & Segal, D. M. (1981) *Biochemistry 20*, 6326.

Hellen, E. H., Fulbright, R. M., & Axelrod, D. (1988) in *Spectroscopic Membrane Probes* (Loew, L. M., Ed.) p 47, CRC Press, Inc., Boca Raton, FL.

Hibbs, M. L., Walker, I. D., Kirszbaum, L., Pietersz, G. A., Deacon, N. J., Chambers, G. W., McKenzie, I. F. C., & Hogarth, P. M. (1986) *Proc. Natl. Acad. Sci. U.S.A. 83*, 6980.

Hibbs, M. L., Classon, B. J., Walker, I. D., McKenzie, I. F. C., & Hogarth, P. M. (1988) *J. Immunol. 140*, 544.

Hogarth, P. M., Hibbs, M. L., Bonadonna, L., Scott, B. M., Witort, E., Pietersz, G. A., & McKenzie, I. F. C. (1987) *Immunogenetics 26*, 161.

Hunziker, W., Koch, T., Whitney, J. A., & Mellman, I. (1990) *Nature 345*, 628.

Kalb, E., Engel, J., & Tamm, L. K. (1990) *Biochemistry 29*, 1607.

Lanni, F., Waggoner, A. S., & Taylor, D. L. (1985) *J. Cell Biol. 100*, 1091.

Lewis, V. A., Koch, T., Plutner, H., & Mellman, I. (1986) *Nature 324*, 372.

Lok, B. K., Cheng, Y. L., & Robertson, C. R. (1983) *J. Colloid Interface Sci. 91*, 87.

McConnell, H. M., Watts, T. H., Weis, R. M., & Brian, A. A. (1986) *Biochim. Biophys. Acta 864*, 95.

Mellman, I. S., & Unkeless, J. C. (1980) *J. Exp. Med. 152*, 1048.

Mellman, I., Koch, T., Healey, G., Hunziker, W., Lewis, V., Plutner, H., Miettinen, H., Vaux, D., Moore, K., & Stuart, S. (1988) *J. Cell Sci., Suppl. 9*, 45.

Miettinen, H. M., Rose, J. K., & Mellman, I. (1989) *Cell 58*, 317.

Mishell, B. B., & Shiigi, S. M. (1980) in *Selected Methods in Cellular Immunology*, p 295, W. H. Freeman and Co., San Francisco.

Nygren, H., & Stenberg, M. (1989) *Immunology 66*, 321.

O'Grady, J. H., Looney, R. J., & Anderson, C. L. (1986) *J. Immunol. 137*, 2307.

Palmer, A. G., & Thompson, N. L. (1989) *Proc. Natl. Acad. Sci. U.S.A. 86*, 6148.

Pecht, I. (1982) in *The Antigens VI* (Sela, M., Ed.) p 1, Academic Press Inc., New York.

Pisarchick, M. L., & Thompson, N. L. (1990) *Biophys. J. 58*, 1235.

Poglitsch, C. L., & Thompson, N. L. (1990) *Biochemistry 29*, 248.

Puré, E., Witmer, M. D., Lum, J. B., Mellman, I., & Unkeless, J. C. (1987) *J. Immunol. 139*, 4152.

Ravetch, J. V., Luster, A. D., Weinshank, R., Kochan, J., Pavlovec, A., Portnoy, D. A., Hulmes, J., Pan, Y.-C. E., & Unkeless, J. C. (1986) *Science 234*, 718.

Schindler, M., Osborn, M. J., & Koppel, D. E. (1980) *Nature 283*, 346.

Segal, D. M., & Titus, J. A. (1978) *J. Immunol. 120*, 1395.

Smith, B. A., & McConnell, H. M. (1978) *Proc. Natl. Acad. Sci. U.S.A. 75*, 2759.

Sober, H. A., Ed. (1973) in *Handbook of Biochemistry*, 2nd ed., p C-67, CRC Press, Cleveland.

Stenberg, M., & Nygren, H. (1988) *J. Immunol. Methods 113*, 3.

Sui, S., Urumow, T., & Sackmann, E. (1988) *Biochemistry 27*, 7463.

Tendian, S. W., Lentz, B. R., & Thompson, N. L. (1991) *Biochemistry* (submitted for publication).

Thompson, N. L., & Axelrod, D. (1983) *Biophys. J. 43*, 103.

Thompson, N. L., & Palmer, A. G. (1988) *Comments Mol. Cell. Biophys. 5*, 39.

Tilton, R. D., Gast, A. P., & Robertson, C. R. (1990) *Biophys. J. 58*, 1321.

Timbs, M. M., & Thompson, N. L. (1990) *Biophys. J. 58*, 413.

Timbs, M. M., Poglitsch, C. L., Pisarchick, M. L., Sumner, M. T., & Thompson, N. L. (1991) *Biochim. Biophys. Acta* (in press).

Unkeless, J. C. (1979) *J. Exp. Med. 150*, 580.
Unkeless, J. C., Healey, G. A. (1983) *J. Immunol. Methods 56*, 1.
Unkeless, J. C., Scigliano, E., & Freedman, V. H. (1988) *Annu. Rev. Immunol. 6*, 251.
Watts, T. H., Brian, A. A., Kappler, J. W., Marrack, P., & McConnell, H. M. (1984) *Proc. Natl. Acad. Sci. U.S.A. 81*, 7564.
Watts, T. H., Gaub, H. E., & McConnell, H. M. (1986) *Nature 320*, 179.
Weinshank, R. L., Luster, A. D., & Ravetch, J. V. (1988) *J. Exp. Med. 167*, 1909.
Weis, R. M., Balakrishnan, K., Smith, B. A., & McConnell, H. M. (1982) *J. Biol. Chem. 257*, 6440.
Wright, L. L., Palmer, A. G., & Thompson, N. L. (1988) *Biophys. J. 54*, 463.
Young, J. D.-E., Unkeless, J. C., Kaback, H. R., & Cohn, Z. A. (1983a) *Proc. Natl. Acad. Sci. U.S.A. 80*, 1636.
Young, J. D.-E., Unkeless, J. C., Young, T. M., Mauro, A., & Cohn, Z. A. (1983b) *Nature 306*, 186.

Tissue-Type Plasminogen Activator Binds to and Is Inhibited by Surface-Bound Lipoprotein(a) and Low-Density Lipoprotein†

Daniel I. Simon,‡ Gunther M. Fless,§ Angelo M. Scanu,§ and Joseph Loscalzo*,‡

Department of Medicine, Harvard Medical School, Brigham and Women's Hospital, and Brockton/West Roxbury Veterans' Administration Medical Center, Boston, Massachusetts, and Departments of Medicine and Biochemistry and Molecular Biology, The Pritzker School of Medicine, The University of Chicago, Chicago, Illinois

Received November 26, 1990; Revised Manuscript Received February 26, 1991

ABSTRACT: Elevated levels of lipoprotein(a) [Lp(a)] are associated with an increased risk of atherothrombotic disease, but the mechanism(s) by which Lp(a) potentiates atherogenesis is unknown. The extensive homology of apolipoprotein(a) [apo(a)] to plasminogen has led us and others to postulate that Lp(a) may impair fibrinolysis. We have previously shown that Lp(a) inhibits fibrin stimulation of plasminogen activation by tissue-type plasminogen activator (t-PA); however, we and other investigators have been unable to demonstrate direct inhibition of t-PA by Lp(a) in solution. We now report that t-PA binds reversibly and saturably to surface-bound Lp(a) and to low-density lipoprotein (LDL) and that as a result of this binding activation of plasminogen by t-PA is inhibited. The catalytic efficiency (k_{cat}/K_m) of t-PA when bound to polystyrene surface-bound fibrinogen increased 2.9-fold compared to t-PA bound to control wells. When bound to surface-bound Lp(a), however, the catalytic efficiency of t-PA was reduced 9.5-fold compared to t-PA bound to control wells; likewise, by binding to surface-bound LDL, the catalytic efficiency of t-PA was reduced 16-fold compared to the control. Studies with defined monoclonal antibodies suggest that major determinants of t-PA binding are its active site, the LDL receptor binding domain of apolipoprotein B-100 (apoB-100), and apo(a). These data suggest a unique mechanism by which Lp(a) and LDL incorporated in an atheroma can inhibit endogenous fibrinolysis and thereby contribute to the genesis of atherothrombotic disease.

The presence of both thrombus and atheroma in the atherosclerotic vessel wall has been recognized for many years (Haust et al., 1964, 1965), but the molecular and cellular mechanisms by which thrombotic and atherogenic processes interact remain poorly defined. One mechanism by which atherogenic determinants may influence thrombotic events occurring in atheromata involves a unique, highly atherogenic lipoprotein, lipoprotein(a) [Lp(a)].[1] First identified by Berg (1963), Lp(a) is comprised of low-density lipoprotein (LDL) covalently linked through a disulfide bridge from apoB-100 to one or two molecules of a unique apoprotein, apo(a). Lp(a) has been localized to the intima of atherosclerotic lesions (Rath et al., 1989), and elevated levels of Lp(a) (greater than approximately 30 mg/dL) are associated with a significantly increased risk of coronary artery disease (Dahlen et al., 1986; Kostner et al., 1981; Murai et al., 1986; Rhoads et al., 1986). The cDNA of apo(a) has recently been cloned and sequenced and demonstrates a remarkable homology to human plasminogen: it contains a serine protease domain that is 94% homologous with that of plasminogen, one copy of a kringle-5-like region, and 37 copies of kringle-4-like domains (McLean et al., 1988). Despite the structural homology to plasminogen, apo(a) does not generate plasmin-like activity when exposed to plasminogen activators owing to a critical amino acid substitution at the analogous activation site. However, recent work by several groups including our own has supported the view that Lp(a) influences fibrinolysis through its kringle domains. Lp(a) has been shown to inhibit plasminogen binding

† This work was supported in part by grants from the National Institutes of Health (HL40411, HL43344, and HL18577) and by a Merit Review Award from the Veterans' Administration. D.I.S. is the Samuel A. Levine Fellow and recipient of an AHA Fellowship Award with funds contributed to in part by the Massachusetts Affiliate. J.L. is the recipient of a Research Career Development Award from the NIH (HL02273).

* Address correspondence to this author at the Department of Medicine, Brigham and Women's Hospital, 75 Francis Street, Boston, MA 02115.
‡ Department of Medicine, Harvard Medical School, Brigham and Women's Hospital, and Brockton/West Roxbury VA Medical Center.
§ Departments of Medicine and Biochemistry and Molecular Biology, the Pitzker School of Medicine, The University of Chicago.

[1] Abbreviations: Lp(a), lipoprotein(a); apo(a), apolipoprotein(a); LDL, low-density lipoprotein; HDL, high-density lipoprotein; apoB-100, apolipoprotein B-100; t-PA, tissue-type plasminogen activator; PPACK, D-phenylalanyl-L-prolyl-L-arginine chloromethyl ketone hydrochloride; TBS, 10 mM Tris/0.15 M NaCl, pH 7.4; BSA, bovine serum albumin; SDS, sodium dodecyl sulfate; ANOVA, analysis of variance.

0006-2960/91/0430-6671$02.50/0